# Paramagnetic Meissner effect in $MgB_2$ superconductor

J. Horvat. X. L. Wang, S. Soltanian and S. X. Dou,
Institute for Superconducting and Electronic Materials, University of Wollongong, NSW 2522, Australia

**Abstract**
Paramagnetic Meissner effect (PME) was observed for the first time in $MgB_2$ pellets and superconducting cores of the iron sheathed $MgB_2$ wires. As opposed to the Meissner effect, the PME consisted of the paramagnetic dc susceptibility in a limited range of the fields. PME was observed in the field-cooled, but also in the zero-field-cooled susceptibility. The later distinguishes it from the PME in the conventional and high-temperature superconductors. PME in $MgB_2$ is in a metastable state connected with the vortex pinning. It cannot be described by the models commonly used for PME in the conventional and high-temperature superconductors. Instead, it is in good agreement with a model based on self-consistent solutions of Ginzburg-Landau equations for a finite size superconductor.

## 1. Introduction

One of the basic properties of a superconductor is the Meissner effect. It consists of the screening of the external field out of the superconducting volume, whereby persistent currents flowing in a limited volume of the superconductor produce the field opposite to the external field. Therefore, the superconductors are diamagnetic materials. However, experiments revealed this need not always be so. A number of conventional and high-temperature superconductors exhibit a paramagnetic moment when cooled in small magnetic fields. This is usually referred to as the paramagnetic Meissner effect (PME). Over the time it became clear that there could be several mechanisms for PME.

PME observed in conventional superconductors is usually explained by the creation of a giant vortex state as the sample is cooled in magnetic field from above its critical temperature $T_c$[1, 2]. This is connected with the existence of the surface critical field $H_{c3}$, which is larger than the bulk critical field $H_{c2}$. Both, $H_{c2}$ and $H_{c3}$ decrease with temperature. If a constant magnetic field is present upon cooling, it penetrates the whole sample for $H>H_{c3}$. As the temperature decreases, the condition $H_{c2}<H<H_{c3}$ occurs, where the superconducting currents start circulating on the circumference of the sample, whilst there is still a homogeneous field present in the non-superconducting bulk. This resembles a giant vortex of the size of the sample itself[3], resulting in a paramagnetic response of the sample upon cooling in magnetic field. The surface currents are very sensitive to the surface treatment of the sample and can be easily eliminated by rough mechanical surface treatment, oxidation, or absorption of the gases on the surface.

A similar model was devised for high temperature superconductors[4], where instead of surface superconductivity, uneven cooling was considered. As a sample is cooled in magnetic field, its surface is at a slightly lower temperature than the bulk because of finite heat conduction through the sample. Because of this, its surface goes through the superconducting transition before the bulk, creating the persistent currents on the perimeter of the sample, which entrap the magnetic flux inside the superconductor. With further cooling, the superconducting boundary moves inward from the surface, compressing magnetic flux. According to the model, this can result in the paramagnetic Meissner effect.

PME for high-temperature superconductors is often cited as a proof of d-wave superconductivity in these superconductors[5, 6]. In this model, Josephson junctions in high-temperature superconductors consist of d-wave functions of opposite phase at the junction interface. Therefore, charge carriers crossing such Josephson junctions experience a phase

shift of π, creating inverse Josephson coupling. In multiply connected superconducting samples with π junctions, this results in spontaneous paramagnetic moments if the values of Josephson currents are large enough.

The paramagnetic π junctions can also be obtained if the Cooper pairs tunnel through Josephson junctions containing magnetic impurities[7, 8]. This model results in the same phenomenology as the d-wave pairing model. An important feature of the spontaneous paramagnetic moments is that, once created, they are rather inert to external changes. This is in contrast to the ordinary metastable moments caused by the vortex pinning.

PME can also be observed as a result of granularity of the sample[9, 10]. In these models, a superconductor is modelled by a system of multiply connected Josephson junctions. When Josephson junctions are suppressed by magnetic field upon cooling through $T_c$ the currents circulate around each of the superconducting volumes separated by the suppressed Josephson junctions[10]. The thickness of the junctions is negligible, as compared to the size of the superconducting volumes. The currents at each side of such junctions flow in the opposite directions, effectively cancelling out each other. The remaining currents effectively correspond to the diamagnetic currents on the perimeter of the sample and paramagnetic currents on the inner edge of the screening volume, i.e. at the penetration depth.

In this paper, we report for the first time that PME also exists in the new $MgB_2$ superconductor. Studying the occurrence of the paramagnetic moment upon cooling in the field, we show that PME in $MgB_2$ is different than in high-temperature superconductors and it does not occur merely as a consequence of inhomogeneous cooling across the transition temperature, or Josephson junctions. Instead, our results support a recent model based on the self-consistent solution of Ginzburg-Landau equations for a finite size superconductor. In this model, PME is a bulk effect and it is caused by the presence of magnetic vortices inside the superconductor. However, PME occurs only if there are metastable superconducting states, resulting in magnetic irreversibility. Our experimental results show that PME for $MgB_2$ is consistent with this model, which indicates that PME for $MgB_2$ is different than the PME usually observed for conventional and high-temperature superconductors of macroscopic size.

## 2. Experimental details

The measurements were performed on a number of $MgB_2$ samples, including four sintered pellets, three iron-sheathed and one silver-sheathed wire. The samples were prepared from the mixture of fine high-purity powders of magnesium and amorphous boron. The powder mixture was either made into pellets, or filled into iron or silver tubes. The superconducting $MgB_2$ was formed in a heat treatment in argon atmosphere at temperatures between 800 and 840°C, depending on the sample. A detailed description of the sample preparation can be found elsewhere [11,12,13]. Critical current densities for thus obtained samples were of the order of $10^5$ A/cm$^2$ at 20K and zero field. Scanning electron microscope examination revealed that the pellets consisted of 200μm size grains, which were agglomerates of single crystals. The grain size in the wires, however, was about 100nm. The critical temperature ($T_c$) was obtained from ac susceptibility measurements, using excitation field with amplitude of 1 Oe and frequency 117Hz. All the samples had $T_c$ of 38K ± 0.5 K.

The iron sheath was removed from the iron sheathed wires before the measurements, making sure there was no remnants of the iron left on the samples. However, there was always a slight contamination of iron present in the superconducting core. Measurements of magnetic hysteresis loops near critical temperature (T>35K) showed a small, but clear ferromagnetic contribution. From the value of magnetic moment in the saturation (for H=2T), we calculated there was about 140 ppm of iron present in our samples. Results of ICP-optical emission spectroscope gave the iron content of 100ppm for our samples[11], which is in agreement with the results obtained from the saturated magnetic moment. Our iron contamination is one order of magnitude less than the contamination reported elsewhere[14], but it still gave a detectable signal above 30K. For lower temperatures, the contribution of the ferromagnetic loop was negligible in

comparison with the loop of the superconductor.

The samples were characterised by measuring the magnetic ac susceptibility and magnetic hysteresis loops, using a Quantum Design PPMS extraction magnetometer/ac susceptometer. The ac susceptibility was measured with the frequency and amplitude of the excitation field of 117Hz and 1Oe, respectively. The critical temperature ($T_c$) was obtained from these measurements as the temperature of the onset of magnetic screening.

Magnetic hysteresis loops were measured at a constant temperature, with the sweep rate of magnetic field of 50 Oe/s. Critical current densities were obtained by using the Beans critical state model for appropriate geometry of the samples [15,16]. In this model, critical current density is proportional to the height of the magnetic hysteresis loop. The irreversibility field ($H_{irr}$) was obtained as the field at which the magnetic moment *m* just becomes reversible, that is, the field above which the value of *m* is the same for ascending and descending magnetic field. In practice, $H_{irr}$ is defined by the uncertainty in measuring the *m*, and therefore the critical current density. In our measurements, $H_{irr}$ was defined as the field above which the critical current density was smaller than 30A/cm$^2$.

The central results in this paper were obtained from the temperature dependence of magnetic moment. Two types of measurements were performed: field-cooled (FC) and zero-field-cooled (ZFC) moment. The FC moment was obtained by switching on a magnetic field at a temperature above $T_c$. The magnetic moment was then measured as the temperature was swept down to 5K, with a constant sweep rate. The ZFC moment was obtained by cooling the sample in zero field from above $T_c$ to 5K. Magnetic field was then switched on, and magnetic moment measured as the temperature was swept up to above $T_c$ with a constant sweep rate. Magnetic dc susceptibility was calculated as $\chi = m/H$.

Because of pinning of magnetic vortices, ZCF and FC moments are not the same below the irreversibility temperature. The temperature above which the difference between the ZFC and FC moment was smaller than the uncertainty in measuring the moment was defined as the irreversibility temperature for that field. This uncertainty corresponds to critical current density of 30A/cm$^2$, the same as for obtaining $H_{irr}$ from the hysteresis loops.

## 3. Experimental results

Figure 1a shows the temperature dependence of dc susceptibility ($\chi = m/H$) for a $MgB_2$ pellet in field-cooled (FC) regime, with H = 0.02, 0.05, 0.1 and 0.3T. The value of $\chi$ is normalised to its value in zero-field-cooled regime for small fields, which represents the full screening of the sample. The temperature was swept with the rate dT/dt=0.5K/min. Figure 1b shows the same for 0.3T, revealing more detail around the superconducting transition temperature $T_c$. As the sample is cooled, $\chi$ starts decreasing, becoming negative at $T_c$. However, $\chi$ starts increasing within 1K below $T_c$, becoming positive and reaching a value almost independent of temperature, $\chi_m$. This shows that $MgB_2$ exhibits the paramagnetic Meissner effect (PME). $\chi_m$ decreases with the field, which is shown in Figure 2. Experimental points in Fig.2 can be fitted by an inverse function:

$$\chi_m = 1/(1.8+H/H_0), \qquad (1)$$

where $H_0 = 5.5\times10^{-5}$T.

Figures 1a and 1b also show the zero-field-cooled (ZFC) branches of $\chi$ vs. temperature. The difference between the ZFC and FC branches shows the magnetic moment of the sample is irreversible, which is a consequence of the vortex pinning. The temperature at which ZFC and FC branches meet is the irreversibility temperature ($T_{irr}$). Figure 1b shows that $T_{irr}$ for H<0.3T is between $T_c$ and the temperature at which $\chi$ just reaches its maximum value $\chi_m$. This is one of the features that distinguishes PME in $MgB_2$ from high temperature superconductors: the ZFC branch in $MgB_2$ can also attain a positive value (Fig. 1b).

As the field increases, the difference between $T_c$ and $T_{irr}$ for that particular field increases. At some value of the field, $\chi$ is no longer constant at low temperatures. Instead, after the initial increase, it gradually decreases

with decreasing temperature, forming a peak in $\chi$ vs. temperature (Figure 3a). The values of $\chi$ on the peak are still positive, until high enough fields are reached. The field above which the peak starts forming is sample dependent and for our samples it varies between 0.3 and 1T. For yet larger fields, the peak shifts to lower temperatures and widens. A characteristic feature of the peak is that the ZFC and FC branches meet at the temperature of the peak, therefore the temperature of the peak coincides with the irreversibility temperature (Fig. 3a).

Influence of the sweep rate of the temperature on the peak in $\chi$ vs. T is shown in Fig.3a for a pellet sample. For $T>T_{irr}$, there is no difference in $\chi$ vs. T for different sweep rates. Both, initial diamagnetic and paramagnetic responses do not depend on the sweep rate of the temperature. However, for $T<T_{irr}$, the FC branch is shifted to positive values of $\chi$ with increasing sweep rate. The ZFC branch, however, shifts to more negative values of $\chi$ with increasing the sweep rate, for temperatures close to the peak. Figure 3b shows the same for a wire, but for low fields for which the peak is still not formed. In the same way as for the higher fields, the value of $\chi_m$ increases with the sweep rate for $T<T_{irr}$. This signifies that PME in $MgB_2$ is a metastable effect, connected with the vortex pinning. Qualitatively the same results were obtained for all other samples measured.

Figure 4 shows the irreversibility field and $H_{c2}$ as a function of temperature for several samples. $H_{c2}$ vs. temperature was obtained as the onset of diamagnetic screening in ZFC and FC branches of the moment vs. temperature, for different fields (open circles, squares and triangles in Fig.4). $H_{c2}$ decreased linearly with temperature for all the measured fields, with $dH_{c2}/dT = - 0.47$ T/K. $H_{irr}$ vs. temperature was obtained as the temperature of the peak in the ZFC and FC branches for different fields. The ZFC and FC branches converged at the temperature of the peak (Fig. 3a). $H_{irr}$ decreased linearly with temperature for all measured samples, with $dH_{irr}/dT = - 0.29$ T/K. The crosses in Fig.4 show $H_{irr}$ vs. temperature obtained from measurements of the magnetic hysteresis loops. The irreversibility field was defined as the field at which the critical current density decreased to 30 A/cm$^2$. Apparently, there is a very good agreement between $H_{irr}$ vs. temperature obtained from the peak in the moment vs. temperature plots and from the magnetic hysteresis loops (Fig.4).

Figure 4 also shows the temperature dependence of the $H_{c2}$ that was obtained as the temperature of inflection in the moment vs. temperature plots, for that particular field (open diamonds)[17]. Reference 17 shows that this lower value of $H_{c2}$ appears as a consequence of anisotropy of the order parameter in $MgB_2$, and it represents $H_{c2}$ for the field oriented along the crystalline c-axis. The higher value of $H_{c2}$ is for the field oriented in the crystalline ab-plane[17]. For the lower $H_{c2}$, $dH_{c2}^{//c}/dT = -0.17$ T/K. This gives the anisotropy parameter $\gamma = H_{c2}^{//ab} / H_{c2}^{//c} = 2.76$. Our value of $\gamma$ is close to the values obtained in the measurements on single crystals, where they range between 1.7 and 2.7 [18,19,20]. However, our value of $\gamma$ is about a half of the value reported in the Reference 17, where the same method for obtaining of $H_{c2}^{//c}$ was used. The values of $H_{irr}$, which correspond to the peak in the moment vs. temperature plots, are higher than $H_{c2}^{//c}$ and lower than $H_{c2}^{//ab}$ (Fig. 4).

## 4. Discussion

The presented experimental results reveal several characteristic features of the paramagnetic Meissner effect in $MgB_2$ samples. The positive FC susceptibility always occurs at temperatures below $T_c$ (Figs 1 and 3). As the value of $T_c$ shifts to lower values with increasing field, so does the temperature at which the positive $\chi$ occurs. For low fields, $\chi$ attains a positive value $\chi_m$ that is almost independent of the temperature (Fig.1). For higher fields, a positive peak in $\chi$ vs. temperature occurs at the irreversibility temperature (Fig. 3a). This peak attains negative values for high fields and it widens with the field. $\chi_m(H)$ is an inverse function of the field (Fig. 2). Positive values of $\chi$ can be obtained for both, ZFC and FC measurements (Figs 1b and 3a). The value of FC susceptibility increases with dT/dt for two combinations of field and temperature. If the field is too small to produce the peak in $\chi$ vs.

temperature, FC susceptibility increases with dT/dt for the temperatures at which $\chi$ has a temperature independent positive value (Fig. 3b). If there is a peak in $\chi$ vs. temperature, FC susceptibility increases with dT/dt for $T < T_{irr}$ (Fig. 3a). The dependence of positive $\chi$ on dT/dt implies that PME is in a metastable state for these combinations of field and temperature. Coincidence between the irreversibility lines obtained from the peak in FC susceptibility and from the hysteresis loop (Fig. 4) also implies that PME is a metastable state connected with the vortex pinning.

The occurrence of the constant positive FC susceptibility for low fields, and the peak in $\chi$ vs. temperature for high fields, can be explained by combined effects of the paramagnetic and diamagnetic screening in the samples. The later is due the conventional screening of external field by the persistent currents at the perimeter of the sample. For low fields, the diamagnetic screening is weak and it saturates within a few Kelvin below $T_c$. When added to the paramagnetic $\chi$ occurring also a few Kelvin below $T_c$, it produces a constant positive $\chi$, providing the diamagnetic $\chi$ is smaller than the paramagnetic one (Fig. 1). For higher fields, the diamagnetic $\chi$ is higher and it develops in a wider temperature range. The paramagnetic $\chi$, on the other hand, decreases with the field. This produces a peak in $\chi$ vs. temperature, as in Fig. 3a. The same basic explanation was given for the Paramagnetic Meissner effect in high-temperature superconductors[21], which is phenomenologically similar to the one in $MgB_2$.

An apparent source of the positive $\chi$ in our samples could be a ferromagnetic or paramagnetic contamination of the samples. Indeed, there is about 140 ppm of iron detected in the samples. However, the contamination cannot account for the measured results. The temperature of the onset of the positive $\chi$ is always related to $T_c$ of $MgB_2$, and this temperature decreases with the field as does $T_c$ (Figs. 1 and 3). The Curie temperature of iron is well above the room temperature, and sharp onset of a positive $\chi$ slightly below $T_c$ of $MgB_2$ cannot be ascribed to the iron contamination. Further, the value of $\chi_m$ extrapolated to zero field would be 0.5 (Eq. 1), whereas the iron should give at least an order of magnitude higher value of dc susceptibility for low fields. If there were a paramagnetic contamination, it would again not give a sharp increase of positive $\chi$ at the transition temperature of $MgB_2$ that changes with magnetic field.

The d-wave coupling[5, 6] and tunnelling of Cooper pairs through the Josephson junction with magnetic impurities[7, 8] can both be ruled out as a possible cause of PME in $MgB_2$. The paramagnetic moments in these two cases are not affected by external changes of field and temperature, once created. On the other hand, the positive moments in $MgB_2$ depend on dT/dt at low temperatures (Figs. 3a and 3b). Further, critical currents in $MgB_2$ are not affected by Josephson junctions. Instead, $MgB_2$ behaves like the conventional metallic superconductors, giving large values of $J_{c0}$ and weak field dependence of $J_c$ [22, 23].

To check if the uneven cooling of the sample and flux compression resulted in the positive $\chi$ [4], the FC and ZFC $\chi$ were measured with different cooling rates. For slower cooling, the sample would have more homogeneous temperature as it undergoes the superconducting transition and the screening currents on the surface would be lower, resulting in a lower value of positive $\chi$. Our measurements (Figs. 3a and 3b) show that $\chi$ is dependent on the cooling rate, however only for the temperatures lower than the temperature of the peak (Fig. 3a), or the temperature of the saturation of the positive $\chi$ (Fig. 3b). For the higher temperatures $\chi$ does not depend on the cooling rate, even if it is positive. If the flux compression was the cause for the positive $\chi$, the cooling rate would affect its value for all temperatures below $T_c$. Our measurements also give a positive $\chi$ in ZFC case for a field range between about 0.1 and 3T, depending on the sample (Figs. 1b and 3a). The flux compression cannot account for the positive ZFC moment because there is no magnetic flux to be entrapped upon the cooling. Small remanent field of the superconducting magnet (up to 1.5 mT) and Earth's field are much smaller than the applied field, and any flux entrapped upon cooling in such small fields would be eliminated by the

subsequent application of much higher field. If the presence of the remanent field upon cooling were responsible for the positive ZFC $\chi$, its influence would be the strongest for the smallest applied fields. The experiment shows the opposite: there is no positive ZFC $\chi$ for applied fields lower than about 0.1T. All this rules out the flux compression as the origin of the PME in our measurements. The change of the value of the positive $\chi$ at low temperatures with the cooling rate is caused by magnetic relaxation after the positive $\chi$ is fully formed upon the field-cooling.

Theoretical models and experiments show that PME can also occur because of multiply connected Josephson junctions[9, 10]. Because Josephson junctions do not play a role in good $MgB_2$ superconductor [22, 23], these models cannot describe PME in $MgB_2$. On the other hand, $MgB_2$ pellets and wires exhibit granular structure, consisting of agglomerates of grains of 100μm and 100nm size, respectively. It was shown that magnetic screening of a whole pellet can break down to the screening of the individual grains at high fields and temperatures [11]. For example, the breakdown starts occurring at 0.2, 3T and 5T for 35, 20 and 5 K, respectively. Magnetic screening around such separated and closely packed grains can give a positive FC $\chi$, similar to the multiply connected Josephson junctions. However, if the grains were decoupled in our measurements, the sample would consist of individually screened grains when cooled in field of 0.3T to 35K, which could produce the positive $\chi_m$ in Fig 1b. On the other hand, the measurements of the field dependence of $J_c$ showed that the grains are beginning to decouple, when cooled in zero field to 35K and then the field of 0.3T is applied (Fig.5 in Ref 11). The pellet samples are an order of magnitude larger than the grains in them. When the sample is cooled to 20K in zero field and then the field of 0.3T is applied, the grains are coupled and whole of the sample is magnetically screened[11]. Calculating $J_c$ from the measured magnetic hysteresis loops, and assuming that the characteristic screening length at 0.3T is of the size of the individual grains for 35K and of the size of the sample for 20K, the value of $J_c$ in the field of 0.3T would be the same at 35 K and 20 K (Fig.5 in Ref. 11). This is highly unlikely and is not consistent with the transport measurements of $J_c$ [24, 25]. Therefore, decoupling of the grains is incomplete at 35K and 0.3T and it cannot be responsible for the positive FC susceptibility reported here. However, if the re-coupling of the grains upon cooling in the field occurs at lower temperatures, it produces a diamagnetic $\chi$, which could be responsible for the occurrence of the peak in Fig 3a if the diamagnetic $\chi$ is larger than the paramagnetic one.

PME in $MgB_2$ cannot be described by the surface superconductivity, either. The giant vortex state caused by the surface superconductivity has been measured only for the samples having smooth and clean surfaces, where the surface critical currents appear below $H_{c3}$ [1-3]. Any surface damage or contamination eliminates the surface currents. The $MgB_2$ samples had rough surfaces and granular structure[11, 12]. Some samples exhibiting PME contained 10% of MgO impurities. The surface currents could not be formed below $H_{c3}$ for such samples.

As described in a recent model[26], the self-consistent solution of Ginzburg-Landau equations for finite size samples predicts the occurrence of the paramagnetic $\chi$ when a superconducting sample is cooled in magnetic field across its critical temperature. In this model, there are two types of the currents circulating in a superconductor placed in a magnetic field. The currents circulating around the vortices inside the superconductor screen out the field in the vortex from the rest of the superconductor and they produce a paramagnetic $\chi$, i.e. the magnetic moment is in the same direction as the external magnetic field. Additional surface currents flow on the perimeter of the sample, screening whole of the sample from the external field. These currents are diamagnetic.

In this model, PME is caused by an imbalance of the currents flowing inside the superconductor[26], as opposed to the models invoking the surface superconductivity for creation of the giant vortex state[1-3]. The role of the sample surface is not crucial here. The model predicts existence of vortex states with different vorticity[26], and each of them can exist

only in a limited range of magnetic fields. Most of the vortex states give diamagnetic $\chi$, but some of them give a paramagnetic $\chi$. If only equilibrium transitions between these states are allowed, no paramagnetic response is possible[26]. However, if metastable states also exist, paramagnetic $\chi$ are allowed, too. The metastable states are introduced in a superconductor by vortex pinning, which is the source of inhomogeneous distribution of the vortices.

According to this model [26], the first state encountered as the superconductor is cooled down in magnetic field across $T_c$ is a diamagnetic state. With further cooling, other states become possible, some of them paramagnetic. The paramagnetic states can exist only within a certain range of magnetic fields and they become diamagnetic for large fields. The PME described by this model is possible only for superconductors larger than a particular size. This size is defined by a parameter[26]:

$$A = \frac{R}{\kappa}\left(\frac{2\pi H}{\Phi_0}\right)^{1/2}, \qquad (2)$$

where $\kappa$ is the Ginzburg-Landau parameter, R is the sample diameter and $\Phi_0$ the flux quantum. For example, for A=1, only diamagnetic $\chi$ is allowed, whereas for larger samples (A=3), paramagnetic $\chi$ is also allowed.

Our experimental results are in good agreement with this model. Upon cooling in magnetic field, all our samples were diamagnetic just below $T_c$ (Figs. 1 and 3). With further cooling, paramagnetic $\chi$ was obtained for small fields. For higher fields, a paramagnetic peak was obtained, which became diamagnetic for yet higher fields (Figs. 1 and 3). The paramagnetic $\chi$ depended on the sweep rate of the temperature, therefore it was in a metastable state. The temperature of the paramagnetic peak in Figure 2a corresponded to the irreversibility temperature (Figs. 3a and 4), confirming that it is connected with the vortex pinning that introduces metastability. To check the sample size effect on the PME, FC $\chi$ was measured for a $MgB_2$ powder, with particle size between 0.2 and 5 $\mu$m. No paramagnetic response was obtained for this powder down to the lowest fields available (2 Oe, as measured by a Hall probe in the magnet). Taking $\kappa = 26$ [22], $R = 5 \times 10^{-4}$ cm, H=100 Oe and $\Phi_0 = 2\times10^{-7}$ Gauss cm$^2$, we obtain for our powder A = 1. Therefore, the model predicts no PME is possible for this powder, just as observed in our measurements. However, the model does not show how the PME develops from diamagnetic state just below $T_c$, nor it describes the ZFC moment.

This model is a very simple one, considering only the case of several vortices. Measurements on mesoscopic superconductors, in which observation of the quantum transitions between the vortex states is possible, support this model[27]. However, similar models were also proposed, which considered macroscopic paramagnetic and diamagnetic currents, and obtained that an average $\chi$ of the superconductor of paramagnetic type can be obtained. For example, Ref. 4 considers the flux compression by uneven cooling, deriving the vortex distribution giving the paramagnetic currents that is similar to the one in Ref.26. The way in which the paramagnetic vortex state is developed is different in Refs. 4 and 26, however the vortex states are the same. This shows that, even though the model in Ref. 26 describes only a small number of vortices, its conclusions can be extended to a large number of vortices, too. Our measurements support the development of the paramagnetic vortex state in $MgB_2$ as described in Ref. 26, and exclude the uneven cooling described in Ref.4.

## 5. Conclusions

Our measurements of dc susceptibility $\chi$ = m/H showed for the first time that a paramagnetic (positive) susceptibility is obtained in a limited range of the fields for $MgB_2$ pellets and Fe sheathed wires. Therefore, $MgB_2$ exhibits the paramagnetic Meissner effect. The paramagnetic susceptibility is in a metastable state and is connected with the vortex pinning. Similarly to the conventional and high-temperature superconductors, the field-cooled $\chi$ is always diamagnetic just below the superconducting

transitions. Paramagnetic $\chi$ is obtained with further cooling of the superconductor. However, the zero-field-cooled $\chi$ can also be paramagnetic, as opposed to the conventional and high-temperature superconductors.

The paramagnetic Meissner effect cannot be explained by the models usually employed for the conventional and high-temperature superconductors. Instead, it is in a good agreement with a model based on self-consistent solution of Ginzburg-Landau equations for cylinder of finite size[26]. In this model, the paramagnetic Meissner effect is caused by the currents flowing inside the superconductor and does not essentially depend on the sample surface, as is the case in the models invoking the surface superconductivity. This model is also in agreement with some observations of the paramagnetic Meissner effect in conventional superconductors[27].

Figure 1: Temperature dependence of the field-cooled (FC) dc susceptibility ($\chi = m/H$) for a $MgB_2$ pellet: a) for different values of the field and b) for H=0.3 T, showing the details around the superconducting transition. The zero-field-cooled branches (ZFC) are also shown.

a)

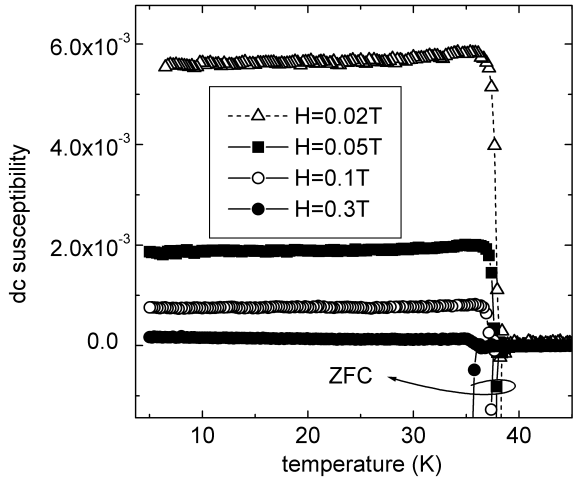


b)

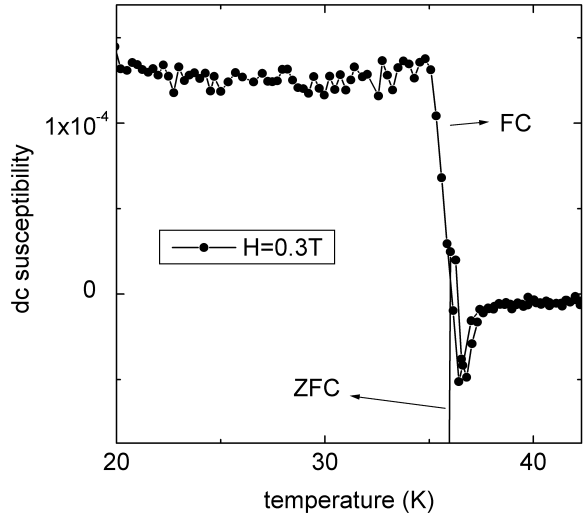

Figure 2: Field dependence of the temperature independent positive $\chi$ for the same sample as in Fig.1.

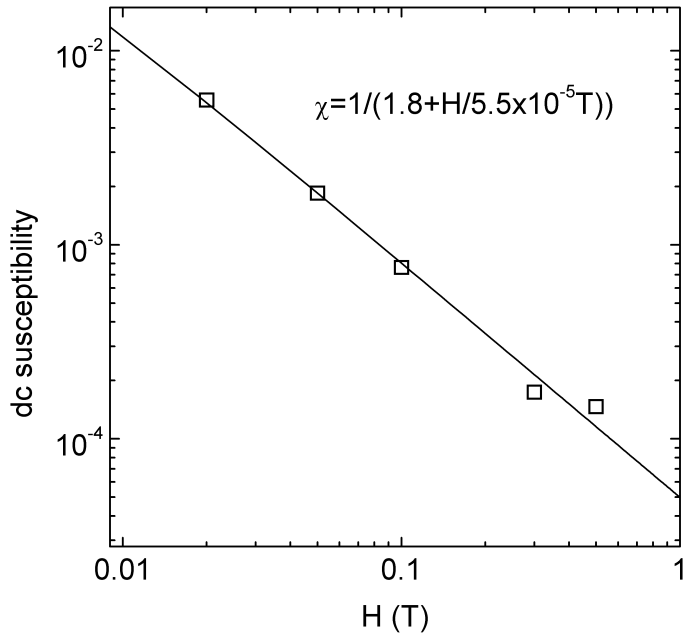

Figure 3:a) Temperature dependence of the field-cooled (FC) dc susceptibility for a $MgB_2$ pellet, with different cooling rates. The fields are higher than in the Figure 1, producing the peak. b) The same for an iron sheathed wire, with fields small enough not to produce the peak. The iron sheath was removed. Zero-field-cooled (ZFC) branches are also shown.

a)

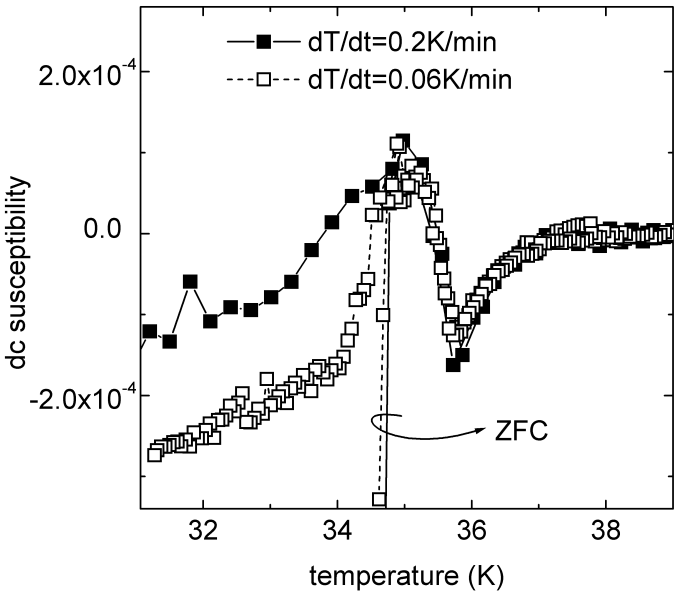


b)

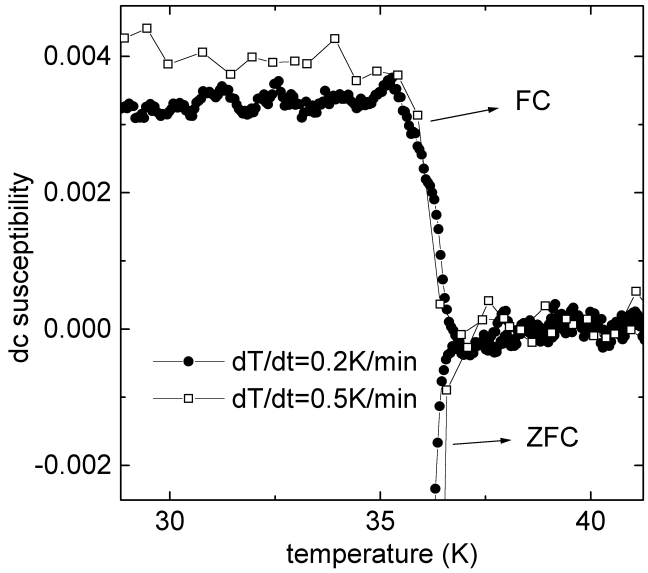

Figure 4: Temperature dependence of the upper critical field ($H_{c2}$) and irreversibility field ($H_{irr}$), shown respectively by open and solid symbols. Different symbols show the data for various samples. This $H_{c2}$ corresponds to the field oriented in the crystalline ab-plane[17]. The values of $H_{irr}$ were obtained from the measurements of zero-field cooled (ZFC) and field cooled susceptibility. Crosses show the irreversibility fields obtained from the hysteresis loops at constant temperature, using the same criterion for definition of $H_{irr}$ as in measurements of zero-field cooled and field-cooled dc susceptibility. The diamonds show the value of $H_{c2}$ corresponding to the field oriented in the crystalline c-axis[17]

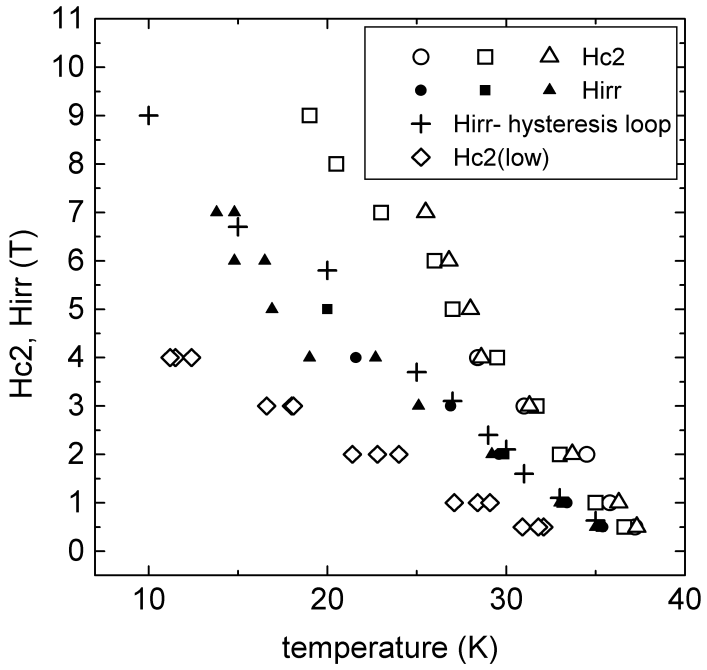

[1] F. de la Cruz, H. J. Fink and J. Luzuriaga, Phys. Rev. B **20**, 1947 (1979).
[2] H. J. Fink and A. G. Presson, Phys. Rev **151**, 219 (1966).
[3] L. J. Barnes and H. J. Fink, Phys. Letters **20**, 583 (1966).
[4] A. E. Koshelev and A. I. Larkin, Phys. Rev. B **52**, 13559 (1995).
[5] W. Braunisch, N. Knauf, G. Bauer, A. Kock, A. Becker, B. Freitag, A. Grütz, V. Kataev, S. Neuhausen, B. Roden, D. Khomskii, D. Wohlleben, J. Bock and E. Preisler, Phys. Rev. B **48**, 4030 (1993).
[6] M. Sigrist and T. M. Rice, Rev. Mod. Phys. **67**, 503 (1995).
[7] L. N. Bulaevskii, V. V. Kuzii and A. A. Sobyanin, Solid State Commun. **25**, 1053 (1978).
[8] B. Z. Spivak and S. A. Kivelson, Phys. Rev. B **43**, 3740 (1991).
[9] W. A. Ortiz, P. N. Lisboa-Filho, W. A. C. Passos, F. M. Araujo-Moreira, Physica C **361**, 267 (2001).
[10] A. P. Nielsen, A. B. Cawthorne, P. Barbara, F. C. Wellstood, C. J. Lobb, R. S. Newrock and M. G. Forrester, Phys. Rev. B **62**, 14380 (2000).
[11] S. X. Dou, X. L. Wang, J. Horvat, D. Milliken, A. H. Li, K. Konstantinov, E. W. Collings, M. D. Sumption and H. K. Liu, Physica C **361**, 79 (2001)
[12] X. L. Wang, S. Soltanian, J. Horvat, A. H. Li, M. J. Qin, H. K. Liu and S. X. Dou, Physica C **361**, 149 (2001).
[13] A. H. Li, X. L. Wang, M. Ionescu, S. Soltanian, J. Horvat, T. Silver, H. K. Liu and S. X. Dou, Physica C **361**, 73 (2001).
[14] O. F. de Lima, R. A. Ribeiro, M. A. Avila, C. A. Cardoso and A. A. Coelho, Phys. Rev. Lett. **86**, 5974 (2001).
[15] C. P. Bean, Phys. Rev. Lett. **8**, 250 (1962).
[16] D. X. Chen and R. B. Goldfarb, J. Appl. Phys. **66**, 2489 (1989).
[17] S. L. Bud'ko, V. G. Kogan and P. C. Canfield, arXiv:cond-mat/0106577, preprint
[18] C. U. Jung, M. S. Park, W. N. Kang, M. S. Kim, S. Y. Lee and S. I. Lee, Physica C **353**, 162 (2001).
[19] M. Xu, H. Kitazawa, Y. Takano, J. Ye, K. Nishida, H. Abe, M. Matsushita and G. Kido, cond-mat/0104366 (2001), preprint.
[20] S. Lee, H. Mori, T. Masui, Yu. Eltsev, A. Yamamoto, S. Tajima, cond-mat/0105545 (2001), preprint.
[21] S. Riedling, G. Bräuchle, R. Lucht, K. Röhberg, H. v. Löhneysen, H. Claus, A. Erb, G. Müller-Vogt, Phys. Rev. B **49**, 13283 (1994).
[22] D. K. Finnemore, J. E. Ostenson, S. L. Bud'ko, G. Lapertot and P. C. Canfield, Phys. Rev. Lett. **86**, 2420 (2001)
[23] D. C. Larbalestier, M. O. Rikel, L. D. Cooley, A. A. Polyanskii, J. Y. Jiang, S. Patnaik, X. Y. Cai, D. M. Feldmann, A. Gurevich, A. A. Squitieri, M.T. Naus, C. B. Eom and E. E. Hellstrom, Nature **410**, 186 (2001).
[24] J. Horvat, X. L. Wang, S. Soltanian and S. X. Dou, Appl. Phys. Lett., submitted.
[25] S. Soltanian, X. L. Wang, I. Kusevic, E. Babic, A. H. Li, M. J. Qin, J. Horvat, H. K. Liu, E. W. Collings, E. Lee, M. D. Sumption and S. X. Dou, Physica C **361**, 84 (2001).
[26] G. F. Zharkov, Phys. Rev. B **623**, 214502-1 (2001)
[27] A. G. Geim, S. V. Dubonos, J. G. S. Lok, M. Henini and J. C. Maan, Nature **396**, 144 (1998).